

Searches for Heavy Diboson Resonances at $\sqrt{s} = 13$ TeV with the ATLAS Detector

Andreas Sogaard*

On behalf of the ATLAS Collaboration

University of Edinburgh (GB)

E-mail: andreas.sogaard@cern.ch

A combined search for high-mass resonances decaying to WW , WZ , and ZZ final states with jets in boosted topologies is presented. The combination comprises four individual searches in the $vvqq$, $lvqq$, $llqq$, and $qqqq$ final states, performed in pp collision data corresponding to an integrated luminosity of 3.2 fb^{-1} at $\sqrt{s} = 13$ TeV collected by the ATLAS detector at the CERN Large Hadron Collider (LHC). Exclusion limits on the heavy resonance production cross section times branching fraction to dibosons are set at the 95% confidence level for three benchmark signal models. The combined search finds upper exclusion limits on the masses of a scalar singlet, a heavy vector-boson triplet, and a Randall-Sundrum graviton at 2650, 2600, and 1100 GeV, respectively.

Fourth Annual Large Hadron Collider Physics

13-18 June 2016

Lund, Sweden

*Speaker.

1. Introduction

Several models beyond the Standard Model (BSM) predict resonances decaying to pairs of vector bosons: WW , WZ , ZZ . Such resonances may be produced in pp collisions at the Large Hadron Collider (LHC) [1]. The vector bosons in turn decay either leptonically, as $W \rightarrow \ell\nu$ or $Z \rightarrow \ell\ell/\nu\nu$, or hadronically, to pairs of quarks $W/Z \rightarrow qq$. The experimental signature of the diboson resonances therefore contains some combination of charged leptons (ℓ), missing transverse energy E_{\perp}^{miss} (ν), and/or hadronic jets (q).

Four searches for such heavy diboson resonances in final states with jets — $\nu\nu qq$, $\ell\nu qq$, $\ell\ell qq$, and $qqqq$ — have been carried out in pp collision data corresponding to a total integrated luminosity of 3.2 fb^{-1} at a center of mass energy of $\sqrt{s} = 13$ TeV, collected by the ATLAS experiment [2] in 2015. The results are interpreted in terms of spin-0 (scalar singlet), spin-1 (heavy vector-boson triplet; HVT), and spin-2 (bulk Randall-Sundrum graviton; G*) benchmark signal models. A combined search in all four final states is performed to improve the sensitivity to BSM physics. Detailed descriptions of the individual searches are presented in Refs. [3, 4, 5, 6], and the combined search is detailed in Ref. [7].

2. Analysis strategy

All four searches focus on high-mass resonances which result in high- p_{\perp} , or “boosted”, final state topologies, reconstructing hadronically decaying bosons as single, trimmed anti- k_t $R = 1.0$ jets, denoted here as J , see Figure 1. Signal “ W/Z jets” jets are selected by requiring the reconstructed mass of the large-radius jet to be within 15 GeV of the W or Z pole mass, respectively. In addition, the W/Z jets are required to pass a p_{\perp} -dependent $D_2^{\beta=1}$ [8] substructure variable cut at a 50% signal efficiency working point. The $D_2^{\beta=1}$ variable is the ratio of 3- to 2-point energy correlation functions on the jet, optimally separating 1- and 2-prong jets; i.e. it is theoretically optimal for separating W/Z jets from jets originating from a single parton (q/g), which enter in most of the major backgrounds. Overlapping W and Z signal regions (SR) are defined by selecting large-radius jets passing the W - and/or Z -jet selection. The selection cuts in each of the four searches are summarised in Table 1.

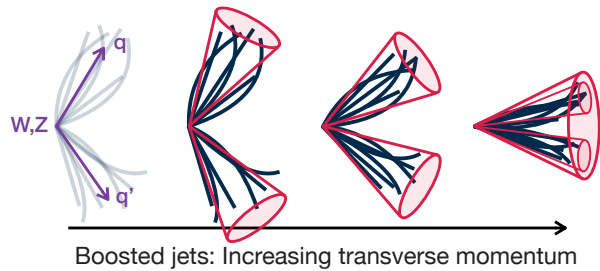


Figure 1: Illustration of the effect of increased transverse momentum on the angular separation of a two-pronged hadronic system (lines), e.g. one originating from the hadronic decay of a vector boson W/Z into two quarks, qq' . At low W/Z p_{\perp} , the quarks can be resolved by reconstructing the vector boson with a small-radius jet algorithm (small cones). At high p_{\perp} the quarks become too collimated to be resolved and are reconstructed as a single, large-radius jet (large cone).

Table 1: Summary of the selection used in each of the four searches for heavy diboson resonances in final states with jets: $\nu\nu qq$, $\ell\nu qq$, $\ell\ell qq$, and $qqqq$ [3, 4, 5, 6]. m_X denotes the invariant mass of the measured final state X , e.g. of the $\ell\ell J$ system. m_\perp is the transverse mass of E_\perp^{miss} and J . See text for details.

Channel	$\ell\ell qq$	$\ell\nu qq$	$\nu\nu qq$	$qqqq$
Trigger type	Single e/μ	E_\perp^{miss} or single e	E_\perp^{miss}	Large- R jet
N_{jet}	≥ 1	≥ 1	≥ 1	≥ 2
$N_{\text{lep.}}$	2	1	0	0
E_\perp^{miss}	—	> 100 GeV	> 250 GeV	< 250 GeV
Topology	$p_{\perp, \ell\ell}/m_{\ell\ell J} > 0.4$ $p_{\perp, J}/m_{\ell\ell J} > 0.4$ $m_{\ell\ell} \approx m_Z$	$p_{\perp, \ell\nu}/m_{\ell\nu J} > 0.4$ $p_{\perp, J}/m_{\ell\nu J} > 0.4$ b -jet veto	$ \Delta\phi(E_\perp^{\text{miss}}, J) > 0.6$	dijet p_\perp balance $ \Delta y(J, J) < 1.2$
Discriminant	$m_{\ell\ell J}$	$m_{\ell\nu J}$	m_\perp	m_{JJ}

After signal region selections, the background composition in each of the four final states and the methods for determining and constraining the background contamination are as follows:

$\ell\ell qq$: Dominated by inclusive Standard Model (SM) $Z \rightarrow \ell\ell$ events (“ Z + jets”; ca. 90% of the total background), constrained using a dedicated control region in the m_J sidebands.

$\ell\nu qq$: Dominated by inclusive $W \rightarrow \ell\nu$ (“ W + jets”; 54%) and SM top processes (34%), constrained using dedicated control regions in the m_J sidebands and by inverting the b -jet veto (i.e. requiring ≥ 1 b -jet), respectively.

$\nu\nu qq$: Dominated by inclusive Z (43%), inclusive W (30%), and top processes (19%), each constrained using the above control regions.

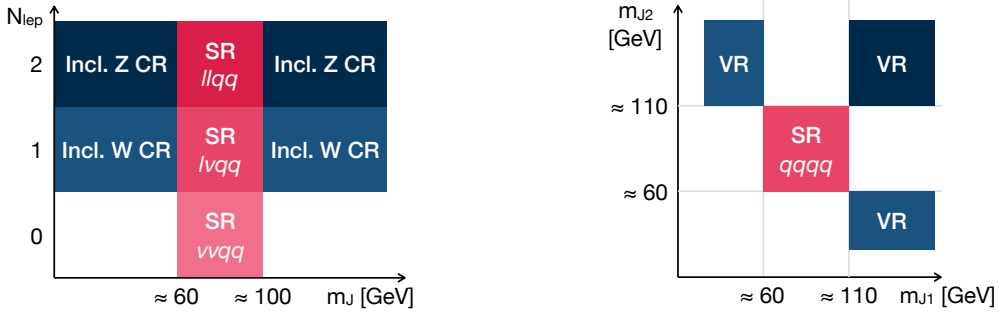
$qqqq$: Completely dominated by SM QCD multijet events, determined using a functional fit to the final discriminant distribution in the signal region(s). The functional form is validated in the sidebands of the leading and subleading jet masses.

In addition, all final states contain some sub-leading background contribution from irreducible SM continuum diboson production. The signal-, control-, and validation regions used in the four analyses are schematically shown in Figure 2(a) and Figure 2(b).

3. Results and combination

Good overall agreement between data and expected background is seen in all final discriminant distributions, with no significant excesses observed in any channel. As examples, Figure 3(a) and Figure 3(b) show the final m_\perp and $m_{\ell\ell J}$ distributions in the ZW signal region for the 0- and 2-lepton channels, $\nu\nu qq$ and $\ell\ell qq$, respectively.

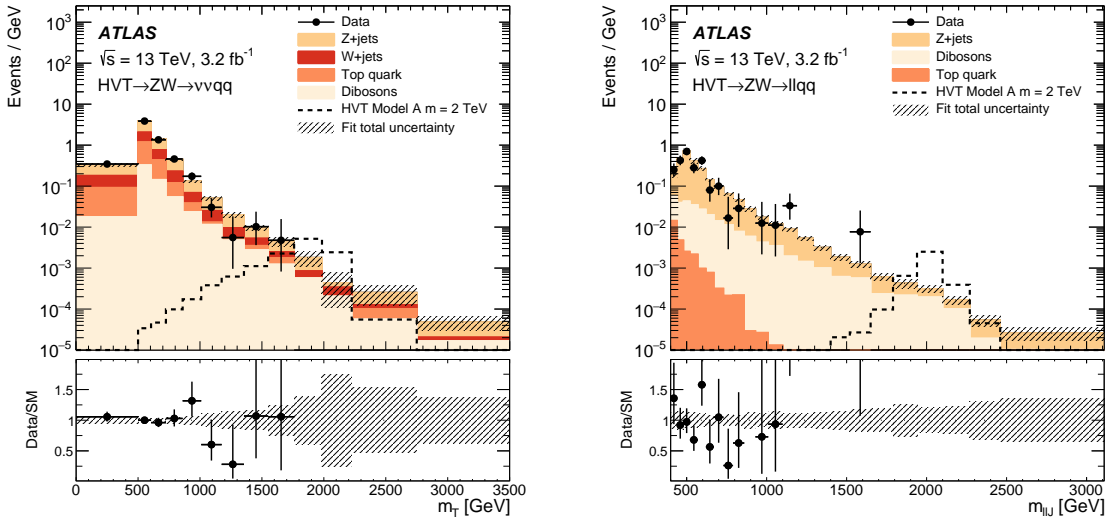
The four individual analyses are combined in a single search [7] by simultaneously fitting all final discriminant distributions in all channels with a single likelihood function. No single channel dominates in terms of sensitivity, justifying a combined search. The frequentist CL_s approach [9] is used to set 95% confidence level cross section exclusion limits as functions of the hypothetical



(a) Signal (SR) and inclusive vector boson control (CR) regions for the semi-leptonic channels, partitioned by leading jet mass m_J and number of signal leptons N_{lep} .

(b) Signal (SR) and non-resonant validation (VR) regions for the fully hadronic channel, partitioned by leading- and subleading jet mass m_{J1} and m_{J2} .

Figure 2: Structure of the signal-, control-, and validation regions for each of the four searches for heavy diboson resonances in final states with jets: (a) $vvqq$, $lvqq$, $llqq$, and (b) $qqqq$ [3, 4, 5, 6]. See text for details.



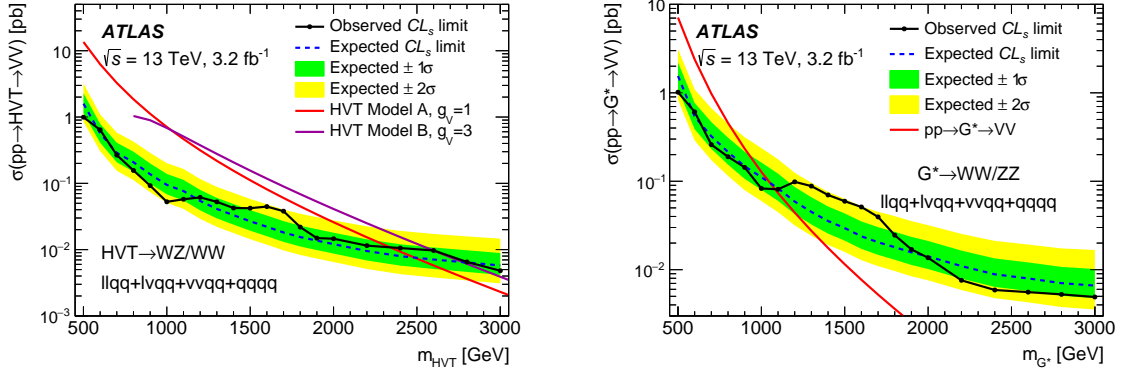
(a) Transverse mass of E_{\perp}^{miss} and large radius jet J in the vvJ channel.

(b) Invariant mass of two signal leptons and large radius jet J in the llJ channel.

Figure 3: Final discriminant distributions for the (a) 0- and (b) 2-lepton final states in the ZW signal region with 3.2 fb^{-1} of data at $\sqrt{s} = 13$ TeV. The shaded, stacked histogram shows the expected contribution from each SM background; the markers are the observed number of events in data; and the dashed line shows the expected contribution from one signal model (charged HVT with a mass of 2 TeV). Figures from [7].

resonance mass, as shown in Figure 4(a) and Figure 4(b) for the HVT and G^* benchmark models, respectively.

No significant excess is found in the combined search. Upper exclusion limits on resonance masses of 2650, 2600, and 1100 GeV are set for the spin-0, spin-1, and spin-2 models, respectively. The presented results display an improvement in sensitivity by a factor of two at resonance masses



(a) HVT decays $W' \rightarrow WZ$ and $Z' \rightarrow WW$, with predicted cross section times branching fraction overlaid.

(b) Bulk RS G^* decays to WW and ZZ , with predicted cross section times branching fraction overlaid.

Figure 4: Expected (dashed line; bands represent expected local ± 1 and 2σ deviations) and observed (markers) 95% CL exclusion limits on the cross section times branching fraction to diboson final states, as functions of the resonance mass, for the (a) HVT and (b) bulk RS G^* models. Figures from [7].

of 2 TeV relative to Run 1 analyses with 20.3 fb^{-1} at 8 TeV with the ATLAS experiment [10] with only 3.2 fb^{-1} of 13 TeV Run 2 data.

References

- [1] L. Evans and P. Bryant (eds.), *LHC Machine*, JINST **3** (2008) S08001
- [2] ATLAS Collaboration, *The ATLAS Experiment at the CERN Large Hadron Collider*, JINST **3** (2008) S08003
- [3] ATLAS Collaboration, *Search for diboson resonances in the $vvqq$ final state in pp collisions at $\sqrt{s} = 13$ TeV with the ATLAS detector*, ATLAS-CONF-2015-068, cdsweb.cern.ch/record/2114840
- [4] ATLAS Collaboration, *Search for WW/WZ resonance production in the ℓvqq final state at $\sqrt{s} = 13$ TeV with the ATLAS detector at the LHC*, ATLAS-CONF-2015-075, cdsweb.cern.ch/record/2114847
- [5] ATLAS Collaboration, *Search for diboson resonances in the $\ell\ell qq$ final state in pp collisions at $\sqrt{s} = 13$ TeV with the ATLAS detector*, ATLAS-CONF-2015-071, cdsweb.cern.ch/record/2114843
- [6] ATLAS Collaboration, *Search for resonances with boson-tagged jets in 3.2 fb^{-1} of pp collisions at $\sqrt{s} = 13$ TeV collected with the ATLAS detector*, ATLAS-CONF-2015-073, cdsweb.cern.ch/record/2114845
- [7] ATLAS Collaboration, *Searches for heavy diboson resonances in pp collisions at $\sqrt{s} = 13$ TeV with the ATLAS detector*, Submitted to *JHEP* [1606.04833]
- [8] A. J. Larkoski, I. Moulton, and D. Neill, *Power Counting to Better Jet Observables*, *JHEP* **12** (2014) 009 [1409.6298]
- [9] A. L. Read, *Presentation of search results: The $CL(s)$ technique*, *J. Phys.* **G28** (2002) 2693–2704
- [10] ATLAS Collaboration, *Combination of searches for WW , WZ , and ZZ resonances in pp collisions at $\sqrt{s} = 8$ TeV with the ATLAS detector*, *Phys. Lett. B* **755** (2016) 285–305 [1512.05099]